Principles of calculating alignment signals in complex resonant optical interferometers

Yaron Hefetz,* Nergis Mavalvala, and Daniel Sigg

Department of Physics and Center for Space Research, Massachusetts Institute of Technology, Cambridge, Massachusetts 02139

Received July 8, 1996; revised manuscript received November 8, 1996

In the long-baseline laser interferometers that are now under construction to measure gravitational waves, the alignment of the optical components with respect to the incoming laser beam is crucial for maintaining maximum phase sensitivity. We present a basic formalism to calculate the effects of misalignment and beam distortions analytically in an arbitrarily complex optical system, including coupled cavities and Michelson interferometer configurations coupled with cavities. The electromagnetic field is decomposed into a superposition of higher-order Gaussian modes, while misaligned and distorting optical components along with free-space propagators are represented by matrix operators that act on the state vectors in this basis. We show how to deduce useful alignment signals generally, in order to design angular control systems. © 1997 Optical Society of America [S0740-3224(97)01807-9]

Key words: Gravitational-wave observatories, laser interferometer, misalignment of Gaussian beams, LIGO, mode decomposition, optical cavities.

1. INTRODUCTION

Gravitational radiation from astrophysical sources produces a strain in space transverse to the direction of propagation.[1] Since this strain has opposite signs along orthogonal axes, variants of a Michelson interferometer have been proposed to measure it by detecting differential changes in the interferometer arm lengths. A typical interferometer configuration, currently planned for the Laser Interferometric Gravitational-Wave Observatory (LIGO) interferometer,[2] comprises a Michelson interferometer with Fabry–Perot optical cavities in each arm and a partially transmitting recycling mirror between the input laser and the beam splitter [see Fig. 1(d)]. The Fabry–Perot arm cavities increase the changes in phase of the light that are due to arm length changes, and the recycling mirror enhances the signal-to-noise ratio by increasing the circulating light in the interferometer. The optical lengths in the interferometer can be held on resonance by various locking schemes.[3,4] These schemes are typically based either on the Pound–Drever–Hall reflection-locking technique, which was first proposed to hold a Fabry–Perot cavity on resonance,[5,6] or on the Schnupp modulation technique,[7] which requires implementation of a length asymmetry in the Michelson interferometer.

While maintaining the longitudinal separations between the test mass mirrors is crucial for optimizing the intensity of the light circulating in the interferometer, the sensitivity of the interferometer to gravitational-wave strain also depends on the angular alignment of the interferometer with respect to the incoming TEM_{00} laser beam. Misalignment of the optical components of the interferometer with respect to the incident laser light causes light in the fundamental mode of the interferometer to be coupled into higher-order modes. This reduces the amount of power circulating in the arm cavities because of diminished coupling of light into them, resulting in reduced phase sensitivity.[8] The higher-order modes leaking out the signal extraction port of the interferometer result in increased photocurrent and shot noise[2] and effectively lower the contrast of the interferometer, which in turn lowers the light-power incident upon the arm cavities. Both effects compromise the signal-to-noise ratio of the gravitational-wave signal readout. Since misalignments can affect the two arms independently, there is less common mode rejection of fluctuations in the laser power, laser frequency, and input beam jitter for differential misalignments. For these reasons it is crucial to maintain tight angular control of the interferometer mirrors.

In this paper, we present a formalism that can be used to study the problem of misalignment in the LIGO interferometer, with the goal of characterizing the sensitivity of the interferometer to angular misalignment and designing a dynamic scheme for maintaining alignment. The general concept of using the transverse (off-axis) modes of an optical resonator to detect misalignment and mismatch was proposed by Anderson.[9] Variations of this idea in conjunction with phase-sensitive detection were proposed and experimentally demonstrated for simple two-mirror resonators.[10–12] Specifically, Morrison *et al.*[12] used a variant of the Pound–Drever–Hall reflection-locking technique[6] for alignment sensing. This is particularly advantageous because light that is already circulating in the interferometer is used to sense both longitudinal and transverse degrees of freedom, which also ensures that the interferometer is aligned relative to the input light beam. Morrison *et al.* investigated a flat-curved Fabry–Perot cavity; they showed that for an infinitely long cavity an angular misalignment of the flat cavity input mirror produces an alignment signal in the

0740-3224/97/0701597-09$10.00

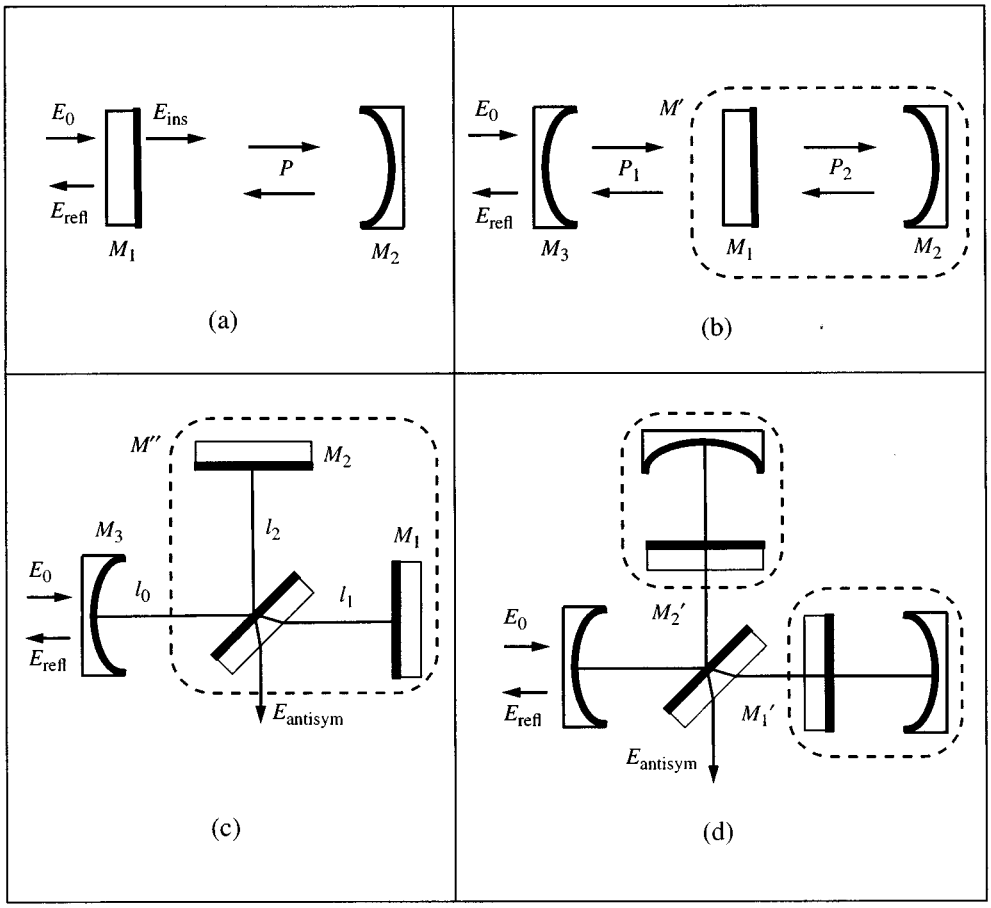

Fig. 1. Setup of (a) a Fabry–Perot interferometer, (b) a coupled pair of cavities, (c) a recycled Michelson interferometer, and (d) a recycled Michelson interferometer with arm cavities.

near field of the light reflected from the input mirror. Similarly, a misalignment of the rear curved mirror produces a signal in the far field.

The present work extends this concept by developing a formalism to analyze more complex optical systems comprising arbitrarily complicated arrangements of optical elements. In particular, it can be applied to systems consisting of cavities placed inside other cavities. The field circulating in the misaligned or distorted optical system is decomposed into a superposition of the eigenmodes of the unperturbed system; the scale of the imperfections or misalignments determines the number of eigenmodes needed for an accurate description. Misaligned or distorting optical components are represented as operators in the basis of these eigenmodes. This approach relies on analytical methods, which gives it tremendous advantage over currently used numerical methods, e.g., the fast Fourier transform,[13,14] which are computationally demanding. For simplicity and tractability we first apply our model to the ubiquitous Fabry–Perot cavity and then build up more complex optical configurations by cascading additional optical elements. We thereby emphasize the generality of the model as an analytical tool for calculating field distortions in any complex optical system.

The formalism for calculating misalignment and distortion operators in the modal space is presented in Section 2. The detection scheme for misalignments is described in Section 3. Section 4 outlines some applications for more complex optical systems, such as coupled cavities and a recycled Michelson interferometer configuration.

2. FORMALISM FOR MODE DECOMPOSITION

The x and y axes of the coordinate system are chosen to be transverse to the beam propagation (and optical axis) of the perfectly aligned and undistorted system (z axis). Using the paraxial approximation,[15] one can quite generally expand the electromagnetic field of a light beam as a superposition of orthonormal Gaussian modes in the form

$$E(x, y, z) = \sum a_{mn} U_{mn}(x, y, z), \tag{1}$$

where a_{mn} can be represented as a vector in the modal space. The $U_{mn}(x, y, z)$ are Gaussian modes, which may be Hermite–Gaussian functions (see examples in Section 4 and the definition in Appendix A). Our goal is to compute the eigenfunctions $U_{mn}(x, y, z)$ only once for the perfectly aligned and undistorted system and then to treat any angular misalignment or distortion as a perturbation that transfers energy only between transverse modes. In other words, the perturbation can be expressed as a matrix operator that acts on a complex vector

space (the modal space), and the solutions to the paraxial wave equation of the misaligned or distorted system can be calculated through a perturbation series approach from the solutions of the unperturbed system.

If $M(x, y, z_2, z_1)$ is an operator that transforms the electromagnetic field of a *misaligned* or distorted optical system at position z_1 into a field at position z_2, i.e.,

$$E'(x, y, z_2) = M(x, y, z_2, z_1) \otimes E(x, y, z_1), \quad (2)$$

its representation $M_{mn,kl}(z_2, z_1)$ in the modal space can be written as

$$M_{mn,kl}(z_2, z_1) = \int \int_{-\infty}^{\infty} U^{\dagger}{}_{mn}(x, y, z_2) M(x, y, z_2, z_1) \times U_{kl}(x, y, z_1) \mathrm{d}x\mathrm{d}y, \quad (3)$$

where the functions $U_{mn}(x, y, z)$ are the eigenmodes of the *unperturbed* system.

An important simplification in calculating the modal space representation of these operators for a real physical system can be obtained through entirely separating the longitudinal propagation from misalignment and distortion effects caused by lenses and mirrors, which affect the wave front only at a fixed longitudinal position.

Since the $U_{mn}(x, y, z)$ are the vacuum eigenmodes, the modal space representation of the propagation operator must be diagonal. In the Hermite–Gaussian basis, e.g., the propagator simplifies to

$$P_{mn,kl}(\eta) = \delta_{mk}\delta_{nl} \exp[-ik(z_2 - z_1)] \times \exp[i(m + n + 1)\eta], \quad (4)$$

where $\eta = \eta(z_2) - \eta(z_1)$ is the Guoy phase shift between position z_2 and z_1 (see Appendix A).

We have included all the rapid longitudinal (z-coordinate) variation in the propagator of the Gaussian beam. The propagator is the only operator that retains a significant z dependence. Hence for lenses and mirrors Eq. (3) reduces to

$$M_{mn,kl} = \langle mn|M(x, y)|kl\rangle \quad (5)$$

where the bra–ket-product is defined as the integration over the transverse degrees of freedom and where $\langle mn|$ and $|kl\rangle$ are the Gaussian eigenmodes with all z dependence that is due to propagation removed.

By calculating the modal space representation of both the propagation and the effects of misalignment, it is possible to calculate the eigenmodes of any misaligned or distorted configuration of the optical system by means of linear algebra only, without repeatedly solving the paraxial wave equation.

Consider a slightly imperfect and slightly misaligned mirror. (The validity of this approximation is clarified below.) Spatial variations over the mirror surface cause each part of the wave front, which is incident at a lateral offset (x, y), to acquire an additional phase shift owing to a local displacement in the z direction (see Fig. 2). The parameters of the unperturbed Gaussian beam are matched to the ideal mirror surface and all deviations from the ideal surface are contained in the function $Z(x, y)$. The mirror distortion operator can then be written as

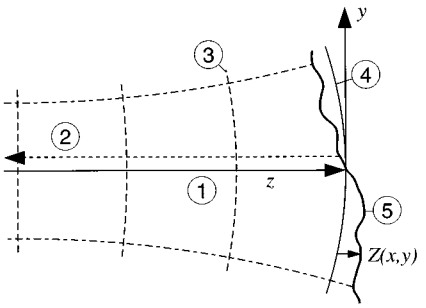

Fig. 2. Reflection on an imperfect and misaligned mirror surface. Direction of ① incoming laser beam, ② reflected beam, ③ undistorted wave front, ④ ideal mirror surface, ⑤ physical mirror surface, $Z(x, y)$, deviation from ideal mirror surface.

$$M(x, y) = \exp[-2ikZ(x, y)]. \quad (6)$$

Generally one has to multiply the right-hand side of Eq. (6) by the reflection coefficient to obtain the true reflected field of the mirror. The distortion operator that describes reflection from the rear surface of the mirror is given by

$$\bar{M}(x, y) = \exp[2ikZ(x, y)] = M^{\dagger}(x, y). \quad (7)$$

If $Z(x, y)$ is a real function, these operators are unitary and thus conserve energy. The modal space representation then becomes[16]

$$M_{mn,kl} = \langle mn|\exp[-2ikZ(x, y)]|kl\rangle = \langle mn|\exp\left(-2ik \sum_{op,qr} |op\rangle Z_{op,qr} \langle qr|\right)|kl\rangle. \quad (8)$$

Since the lateral size of the Gaussian beam is fully described by the spot size, $w(z)$, which is simply a transverse scaling factor, the z dependence of $Z_{op,qr}$ in Eq. (8) can be removed by the variable substitutions $x' = \sqrt{2}x/w(z)$ and $y' = \sqrt{2}y/w(z)$. Expanding $Z(x, y)$ in a series of orthonormal polynomials H_i (such as the Hermite or Zernike polynomials) of the form

$$-2kZ(x, y) = \sum_{i,j} c_{ij} H_i(x') H_j(y'), \quad (9a)$$

one obtains

$$-2kZ_{op,qr} \equiv 2\sum_{i,j} c_{ij} T^{ij}_{op,qr} = \sum_{i,j} c_{ij} \langle op|H_i(x)H_j(y)|qr\rangle|_{z=0}. \quad (9b)$$

The $T^{ij}_{op,qr}$ are Hermitian operators that serve as generators for the unitary transformation that describes the wave front distortion. A detailed calculation of these generators in the Hermite–Gaussian basis is presented in Appendix A.

The physical meaning of the individual terms in the expansion of Eq. (9a)—with Hermite polynomials used in the expansion—can be understood as follows: The constant term, c_{00}, corresponds to longitudinal displacements of the mirror; terms proportional in $H_1(x)$ or $H_1(y)$ and hence linear in x or y correspond to yaw and pitch, respectively, where the coefficients c_{10} and c_{01} are proportional to the rotation angle; the term proportional

to $H_2(x) + H_2(y)$ corresponds to a deviation in the curvature of the spherical phase front; a term proportional to $H_2(x) - H_2(y)$ depicts astigmatism; and so on.

For a small rotation about the y axis $Z(x, y)$ can be written as $Z(x, y) = \theta_x x$. On substitution of $\Theta_x = \theta_x \pi w(z)/\lambda$, which is the normalized rotation angle, the operator becomes

$$-2kZ(x, y) = -\sqrt{8}\Theta_x \frac{\sqrt{2}x}{w(z)} = -\sqrt{2}\Theta_x H_1(x'). \quad (10)$$

In the Hermite–Gaussian basis, the recursion relationship for the Hermite polynomials simplifies the generator T^{10} to

$$T^{10}_{op,qr} = \frac{1}{\sqrt{2}} \delta_{pr}(\sqrt{q}\,\delta_{o,q-1} + \sqrt{o}\,\delta_{o,q+1}). \quad (11)$$

The Hermite–Gaussian basis is particularly well suited to describe small misalignments, as indicated by the simple form of Eq. (11). Notably, if the generator in Eq. (11) is applied to the fundamental TEM_{00} mode, then TEM_{10} is the only resulting mode. Any other higher-order mode that can be excited by a misaligned mirror is introduced only by the matrix exponential of Eq. (8); in other words, other modes are not significant if the normalized rotation angle is small compared with unity.

A similar problem is the distortion of the wave front when it passes through an optical element such as a partially transmitting mirror or a lens. If the deviation in thickness of the optical element from its ideal shape is denoted by $d(x, y)$, then the distortion operator can be written as

$$M(x, y) = \exp[-i(n - 1)k\,\mathrm{d}(x, y)], \quad (12)$$

where n is the refractive index of the optical medium. This operator is of the same form as the distortion operator in reflection, with one exception: The linear term in $d(x, y)$ does not account for an angular tilt, but instead describes a wedge. In fact, an angularly misaligned optical element shifts the beam laterally. For a small tilt θ_x about the y axis, the shift in the x direction can be calculated with Snell's law:

$$\Delta(x) \approx \theta_x\left(1 - \frac{1}{n}\right)d \quad (13)$$

where n and d are the index of refraction and the thickness of the optical element, respectively. A detailed calculation of the lateral shift operator is presented in Appendix A.2.

With regard to optical cavities, tilting the partially transmitting input mirror of the cavity has two effects: First, the wave front of the field inside the cavity is distorted by the tilt of the reflecting surface, and, second, the incident beam is shifted laterally on transmission through the input coupler. When expression (13) is compared with Eq. (10), the effect of lateral shift turns out to be much smaller, roughly by a factor of d/z_0, which is negligible for most practical cavity configurations.

3. DETECTION SCHEME IN THE MODAL PICTURE

The Pound–Drever–Hall reflection-locking scheme[6] is a powerful technique for holding optical cavities and interferometers on resonance. When phase-modulated light is incident upon an optical cavity, then deviation from the resonance length causes amplitude modulation to appear on the light reflected from the cavity. Close to the resonant state, the magnitude of the amplitude modulation is proportional to the deviation from resonance, whereas the sign of the phase gives the direction of deviation from the resonant length and hence can be used as an error signal to hold the cavity on resonance.

The same technique can be used for spatial sensing of the wave front[12] (see Fig. 3). If one of the mirrors of a resonant optical system is misaligned, higher-order transverse modes are excited. As shown in Eqs. (8)–(11), a small misalignment about the y axis excites mostly TEM_{10} mode. For a resonant system that carries phase-modulated light, the amount of excited TEM_{10} mode can be measured by detection of the beating between the TEM_{00} and the TEM_{10} modes from the carrier and its sidebands. A segmented photodetector that is split along the y axis, where the signals from the two half-planes are subtracted from each other, is most sensitive to this beating and at the same time rejects any signal coming from longitudinal misalignments.

Since the different order modes propagate with different Guoy phases, the detected modulation depth also depends on the distance between the photodetector and the cavity or interferometer output. Higher-order modes generated by tilted optical elements that have a longitudinal separation—the input and rear mirrors of a cavity, for example—have to travel different distances to the photodetector and can thus be distinguished with two segmented photodetectors at two different locations.

In the remainder of this section an expression for the demodulated signal is derived for a misaligned optical system in the modal space. If $O(\omega)$ is an operator that depicts an entire optical system and if the incoming laser beam consists of a carrier and a pair of phase-modulation sidebands, for small modulation depths the field at the output of the system can be written as

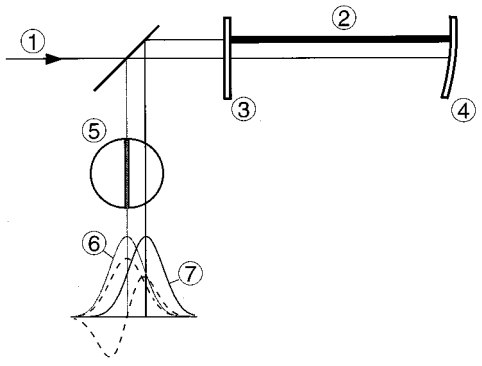

Fig. 3. Alignment signals from a misaligned Fabry–Perot interferometer: ① incoming laser beam, ② resonant cavity mode, ③ partially transmitting input mirror, ④ tilted rear mirror, ⑤ segmented photodetector, ⑥ reflected sideband (gray curve), ⑦ reflected carrier light (solid curve) with its modal decomposition (dashed curve).

$$E_{\text{out}} = E^{\text{CR}} + E^{\text{SB}+} + E^{\text{SB}-}, \tag{14a}$$

$$E^{\text{CR}} = O(\omega_{\text{CR}})E_{\text{inp}},$$

$$E^{\text{SB}\pm} = i\,\frac{\Gamma}{2}\,O(\omega_{\text{CR}} \pm \Delta\omega)E_{\text{inp}}, \tag{14b}$$

where ω_{CR} corresponds to the frequency of the carrier, $\Delta\omega$ is the modulation frequency, Γ is the modulation depth, and E_{inp} is the incident field in the modal space (usually the fundamental mode).

The total light power on the photodetector, which is placed at a distance η in Guoy phase away from the output of the optical system, is

$$\bar{S} = \frac{\epsilon_0 c}{2}\,[P(\eta)E_{\text{out}}]^{\dagger} D^{\Omega}[P(\eta)E_{\text{out}}], \tag{15}$$

where D^{Ω} is an operator that accounts for the physical dimensions of the photodetector, $P(\eta)$ is the propagator defined in Eq. (4), and ϵ_0 and c are the permittivity of free space and the speed of light, respectively. If $\bar{S}$ is demodulated with the modulation frequency $\Delta\omega$, then only terms that have an $\exp(-i\Delta\omega t)$ dependence on the modulation frequency remain in the down-converted signal:

$$S = \frac{\epsilon_0 c}{2}\,(E^{\text{CR}})^{\dagger} P^{\dagger}(\eta) D^{\Omega} P(\eta) E^{\text{SB}-}$$

$$+\ \frac{\epsilon_0 c}{2}\,(E^{\text{SB}+})^{\dagger} P^{\dagger}(\eta) D^{\Omega} P(\eta) E^{\text{CR}}. \tag{16}$$

In Appendix A.3 we calculate the demodulation operator D^{Ω} in the modal space for arbitrarily shaped detectors. From the form of the propagator [see Eq. (4)], it can be seen that the η dependence in S can be expressed in terms of a sine and cosine series

$$S = \sum_{s=0}^{\infty} d_s \cos(s\eta) + \sum_{s=0}^{\infty} e_s \sin(s\eta), \tag{17}$$

where the coefficients d_s and e_s are complicated functions of the detector shape and the output fields. They are completely independent of the detector position if the ratio of the beam spot size over the detector diameter is held constant.

The above expansion is helpful in understanding the Guoy phase dependence of the demodulated signal. For instance, a single photodetector that covers the full cross section of the beam has only one nonzero coefficient, d_0. Similarly, d_1 and e_1 are the only significant coefficients for small angular misalignments measured by a half-plane detector, which is split along one axis.

4. APPLICATION TO GENERAL OPTICAL SYSTEMS

The above technique is applied to calculate the alignment signals of a Fabry–Perot cavity [see Figs. 1(a) and 3]. The cavity round-trip propagation in matrix form reads as

$$P_{\text{rt}} = (-r_1)(-r_2)M_1 P M_2 P, \tag{18}$$

where M_1 and M_2 are the misalignment matrices of the front and the rear mirror, respectively, P denotes the propagator between the two mirrors (note that both the plane-wave phase factor and the Guoy phase shift are exactly the same for both beam directions), and r_1 and r_2 are the amplitude reflection coefficients of the two mirrors (we follow the convention that if the light is reflected from the coated surface of a mirror—drawn as bold curve in Fig. 1—an additional factor of (-1) has to be taken into account). The steady-state equation for the field inside the cavity, E_{ins}, can then be written as:

$$E_{\text{ins}} = P_{\text{rt}}E_{\text{ins}} + t_1 E_0 = t_1(I - P_{\text{rt}})^{-1}E_0, \tag{19}$$

and the reflected field becomes

$$E_{\text{refl}} = r_1 M_1{}^{\dagger} E_0 - t_1 r_2 P M_2 P E_{\text{ins}}$$

$$= r_1 M_1{}^{\dagger}\left(I - \frac{r_1{}^2 + t_1{}^2}{r_1{}^2}\,P_{\text{rt}}\right)(I - P_{\text{rt}})^{-1}E_0$$

$$\equiv M' E_0, \tag{20}$$

where t_1 is the amplitude transmission coefficient of the input mirror, E_0 is the input field, and I is the identity matrix.

For small misalignments the only important modes are the fundamental TEM_{00} mode and the lowest-order transverse (Hermite–Gaussian) modes, TEM_{10}, and TEM_{01}. With the notation in which all three modes are the components of a single vector, an electromagnetic field in modal space can be written as

$$E = \begin{bmatrix} a_{00} \\ a_{10} \\ a_{01} \end{bmatrix}. \tag{21}$$

With Eqs. (4) and (11) used and terms only to first order included in Θ_x and Θ_y,[17] the propagator and the mirror misalignment matrices become

$$P(z_2, z_1) = \exp[-ik(z_2 - z_1)]\begin{bmatrix} e^{i\eta} & 0 & 0 \\ 0 & e^{2i\eta} & 0 \\ 0 & 0 & e^{2i\eta} \end{bmatrix},$$

$$M(\Theta_x, \Theta_y) \approx \begin{bmatrix} 1 & -2i\Theta_x & -2i\Theta_y \\ -2i\Theta_x & 1 & 0 \\ -2i\Theta_y & 0 & 1 \end{bmatrix}. \tag{22}$$

Assuming that the incoming light E_0 is a pure phase-modulated TEM_{00} mode with a carrier that is resonant in the Fabry–Perot cavity and with sidebands that are not resonant, the alignment signal S measured with a half-plane detector—as defined in Eqs. (A14) and (A16)—can be obtained from Eqs. (16), (17), and (20). To first order in Θ, S is given by

$$S = S_0\Gamma\,\frac{\epsilon_0 c E_0{}^2}{2}\,[\Theta_{1x}\cos(\eta_0 + \bar{\eta})$$

$$+\ \Theta_{2x}\cos(\eta_0 + \bar{\eta} + \eta)], \tag{23}$$

where $\bar{\eta}$ is the Guoy phase shift that the TEM_{00} mode of the reflected beam acquires between the input mirror and the photodetector. For a Fabry–Perot cavity S_0 and η_0 are complicated functions of r_1, t_1, r_2, and η. An attractive feature of Eq. (23) is that if additional higher-order modes are included in its derivation they contribute to the order of Θ^3 or higher only. This is illustrated in Fig. 4,

where the angular error signal S and the electromagnetic-field strength of the modes inside the cavity are plotted against the misalignment angle of the front mirror, Θ_{1x}. The calculations were made with only one transverse degree of freedom. It can be seen that the first-order approximation (2 modes) is in good agreement with the exact solution (22 modes) up to normalized angles of 0.3. Cavity parameters of a typical LIGO arm cavity were used, with a cavity length of 4 km, radii of curvature for the input and rear mirror of $-14{,}500$ km and 7400 km, respectively, a perfectly reflecting rear mirror, and an input mirror with a power transmission of 3%.

The Guoy phase η is pivotal to the mode decomposition technique. Each nondegenerate mode of the field has a different propagation phase associated with it, and it is precisely this property that allows us to infer which optical component in the optical train is misaligned. From Eq. (23) it can be seen that the Guoy phase difference of the misalignment signal, generated by the input and rear mirrors of a Fabry–Perot cavity, is the Guoy phase shift acquired by the fundamental mode when propagating from one mirror to the other. This has unfortunate implications for a highly degenerate cavity, for which the misalignment signals from the input and rear mirrors become indistinguishable.

The single-cavity equations can be used to calculate the fields propagating in a pair of coupled cavities. Referring to Fig. 1(b), one can calculate the field reflected from mirror 3 by replacing M_1 and M_2 and their corresponding mirror reflectivities in Eqs. (18) and (19) with M_3 and M', given in Eq. (20); i.e.,

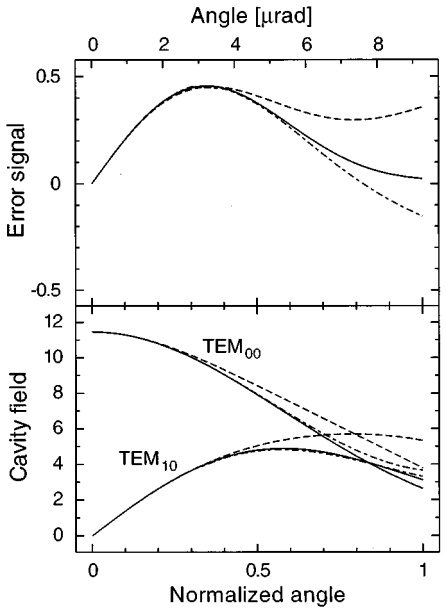

Fig. 4. Angular error signal (top) and mode decomposition (bottom) as a function of the misalignment angle of the front mirror in a resonant Fabry–Perot interferometer. The calculations were made with one transverse degree of freedom only, with 2 modes (dashed curve), 4 modes (dash-dotted curve), and 22 modes (solid curves), respectively. The cavity fields are given in units of the input field, whereas the error signal is given relative to the input power and the modulation depth calculated for the Guoy phase of the detector, which gives the maximum signal at small angles. The cavity parameters are given in the text.

$$E_{\text{refl}} = r_3 M_3{}^{\dagger}\left(I + \frac{r_3{}^2 + t_3{}^2}{r_3} M_3 P_1 M' P_1\right) \times (I + r_3 M_3 P_1 M' P_1)^{-1} E_0, \tag{24}$$

where M_3 and t_3 are the mirror matrix and the amplitude transmission coefficient for mirror 3, respectively, and P_1 and P_2 are the free-space propagators corresponding to the length of each cavity.

Similarly, for a Michelson interferometer with a partially transmitting mirror at the input, as shown in Fig. 1(c), all the complexity of the Michelson interferometer can be contained in a matrix operator M''. The field reflected from the input mirror is then given by

$$E_{\text{refl}} = r_3 M_3{}^{\dagger}\left(I + \frac{r_3{}^2 + t_3{}^2}{r_3} M_3 P_0 M'' P_0\right) \times (I + r_3 M_3 P_0 M'' P_0)^{-1} E_0, \tag{25a}$$

with

$$M'' = -t_{\text{BS}}{}^2 r_1 P_1 M_1 P_1 - r_{\text{BS}}{}^2 r_2 P_2 M_2 P_2, \tag{25b}$$

and the field at the antisymmetric output of the interferometer becomes

$$E_{\text{antisym}} = t_3 r_{\text{BS}} t_{\text{BS}} (-r_1 P_1 M_1 P_1 + r_2 P_2 M_2 P_2) \times (I + r_3 M_3 P_0 M'' P_0)^{-1} E_0, \tag{26}$$

where r_{BS} and t_{BS} are the amplitude reflection and transmission coefficients of the beam splitter.

In this manner, we can piece together any optical system and extract the spatially varying fields at any transverse plane along the direction of propagation of the wave vector. Figure 1(d) shows the optical layout for the complete LIGO interferometer. Fields for this system can be calculated by replacement of $(-r_1 M_1)$ and $(-r_2 M_2)$ in the equations for the simple Michelson interferometer with matrices $M_1{}'$ and $M_2{}'$, which are similar to the cavity operator M' of Fig. 1(b) and Eq. (20).

5. CONCLUSIONS

We have presented the theory of mode decomposition in complex resonant optical interferometers, using a formalism that is versatile, flexible, and easily extensible to include an arbitrary number of higher-order modes. This formalism provides an analytical modeling tool that can be easily adapted for different optical configurations. There is no intrinsic limit on the number of optical components, since the algorithms described in this work are computationally very efficient.

The wave-front-sensing scheme is particularly valuable when applied to gravitational-wave interferometers because it does not require an external reference point (as is the case with auxiliary optical levers, for example); external reference points have the potential to drift relative to the interferometer. Furthermore, the interferometer light already carries phase-modulation sidebands used for the length-sensing system. When a practical scheme is being developed for detecting angular misalignments, not only must the misalignment effect be measurable, but its origin must also be determined. All cases examined to date support the conclusion that if a particular modula-

tion configuration gives reliable information to sense the longitudinal degrees of freedom for the optical system, then probing the spatial dependence of the same light also gives a good misalignment signal. However, determining its origin can be a problem in certain special cases—a highly degenerate Fabry–Perot cavity, for example—since the signals originating from the two mirrors that form the cavity may be indistinguishable.

The modal model described in this work was used as a design and analysis tool to study various configurations of interferometric gravitational-wave detectors, including the complete LIGO interferometer. In particular, we have studied the degradation in sensitivity to gravitational waves of a proposed LIGO interferometer due to angular misalignments.[8] Additionally, we have developed a robust angular control system for the LIGO interferometer based on the wave-front-sensing technique described in this work. Simulations carried out with this model will also play an important role in converging on the optimal modulation configuration for LIGO. A tabletop-scale, prototype interferometer experiment is under way to verify a LIGO-like alignment-sensing scheme.

APPENDIX A: FORMULAS

In this appendix the detailed equations of the modal model formalism are worked out by use of the Hermite–Gaussian representation. In the paraxial approximation, the solutions to the scalar-wave equation in one dimension can be expressed as a superposition of Hermite–Gaussian modes[15]:

$$U_m(x, z) = \left(\frac{2}{\pi}\right)^{1/4}\left(\frac{1}{2^m m! w(z)}\right)^{1/2} H_m\left[\frac{\sqrt{2}x}{w(z)}\right] \times \exp\left\{-x^2\left[\frac{1}{w(z)^2} + \frac{ik}{2R(z)}\right]\right\} \times \exp\left[i\left(m + \frac{1}{2}\right)\eta(z)\right], \tag{A1}$$

where the z axis points in the beam propagation direction and where $\eta(z)$, $w(z)$, and $R(z)$ are the mode-dependent Guoy phase shift, the spot size, and the curvature of the phase front at position z, respectively,

$$\eta(z) = \tan^{-1}\left(\frac{z}{z_0}\right), \quad w(z) = w_0\left[1 + \left(\frac{z}{z_0}\right)^2\right]^{1/2}, \quad R(z) = z + \frac{{z_0}^2}{z}, \tag{A2}$$

and the Rayleigh length, z_0, is given by $z_0 = \pi {w_0}^2/\lambda$, with w_0 the waist size. $H_m(x)$ is the Hermite polynomial of order m. The following relations are used repeatedly in the calculations that follow:

$$\int_{-\infty}^{\infty} {U_m}^{\dagger}(x, z) U_n(x, z)\mathrm{d}x = \delta_{mn}, \tag{A3a}$$

$$2xH_m(x) = H_{m+1}(x) + 2mH_{m-1}(x), \tag{A3b}$$

$$\frac{\mathrm{d}}{\mathrm{d}x} H_m(x) = 2mH_{m-1}(x), \tag{A3c}$$

$$\int_{-\infty}^{\infty} {U_m}^{\dagger}(x, 0) \frac{H_i(\sqrt{2}x/w_0)}{H_k(\sqrt{2}x/w_0)} U_k(x, 0)\mathrm{d}x = \left(\frac{2^i i!}{2^k k!}\right)^{1/2} \delta_{mi}. \tag{A3d}$$

Equation (A3a) is the orthonormality condition; Eqs. (A3b) and (A3c) are recursion relations to be used to derive Hermite polynomials of any order, beginning with $H_0(x) = 1$.

In two dimensions the Hermite–Gaussian modes are given by

$$U_{mn} = U_m(x, z) U_n(y, z)\exp(-ikz), \tag{A4}$$

with the plane-wave phase-shift factor included for completeness.[15]

1. Wave-Front Distortion Operator

The generator for the wave-front distortion operator is given in Eq. (9b). Multiplying the operator, which is given between the bra and ket by $H_q(x)H_r(y)/H_q(x)H_r(y)$, and expanding the numerator as a series of Hermite polynomials, one obtains

$$H_i(x)H_j(y)H_q(x)H_r(y) = \sum_{st} h^{ij}_{st,qr} H_s(x)H_t(y). \tag{A5}$$

Substituting Eq. (A5) back into Eq. (9b) and using (A3d) finally gives

$$T^{ij}_{op,qr} = \frac{h^{ij}_{op,qr}}{2}\left(\frac{2^o o! 2^p p!}{2^q q! 2^r r!}\right)^{1/2}. \tag{A6}$$

In particular, for a simple tilt around the y axis, one gets Eq. (11).

2. Lateral Shift Operator

If a beam is laterally shifted with respect to the direction of propagation, the shift operator $O(\Delta x, \Delta y)$ is defined as

$$E(x + \Delta x, y + \Delta y, z) = O(\Delta x, \Delta y) \otimes E(x, y, z). \tag{A7}$$

Expanding the left-hand side in a Taylor series about x and y gives

$$O(\Delta x, \Delta y) = \exp\left[i\left(\Delta x \frac{1}{i}\frac{\mathrm{d}}{\mathrm{d}x} + \Delta y \frac{1}{i}\frac{\mathrm{d}}{\mathrm{d}y}\right)\right]. \tag{A8}$$

In the modal basis, this unitary operator can be written as

$$O_{mn,kl}(\Delta x, \Delta y) = \langle mn|\exp\left\{i\sum_{op,qr}|op\rangle\left[\frac{\sqrt{2}\Delta x}{w(z)} T^x_{op,qr} + \frac{\sqrt{2}\Delta y}{w(z)} T^y_{op,qr}\right]\langle qr|\right\}|kl\rangle, \tag{A9a}$$

with

$$T^x_{op,qr} = \delta_{pr}\int_{-\infty}^{\infty} \mathrm{d}x {U_o}^{\dagger}(x, z) \frac{w(z)}{i\sqrt{2}} \frac{\mathrm{d}}{\mathrm{d}x} U_q(x, z), \tag{A9b}$$

where the straightforward integration over y is already done. $T^y_{op,qr}$ can be deduced from the right-hand side of Eq. (A9b) by replacing x with y and interchanging the in-

dices o, p with q, r. Once again, the recursion relations of Eq. (A3) are used to solve the integration:

$$H_r\left(\frac{\sqrt{2}x}{w(z)}\right)\frac{w(z)}{i\sqrt{2}}\frac{\mathrm{d}}{\mathrm{d}x}U_r(x,z) = \left[\frac{1}{2}H_{r+1}\left(\frac{\sqrt{2}x}{w(z)}\right)t + rH_{r-1}\left(\frac{\sqrt{2}x}{w(z)}\right)t^*\right]U_r(x,z) \tag{A10a}$$

where

$$t = i - \frac{w(z)^2k}{2R(z)} = i - \frac{z}{z_0}. \tag{A10b}$$

The generator of shifts in x is obtained by Eq. (A3d)

$$T^x_{op,qr} = \frac{1}{\sqrt{2}}\delta_{pr}(\sqrt{o}t\,\delta_{o,q+1} + \sqrt{q}t^*\delta_{o,q-1}). \tag{A11}$$

3. Demodulation Operator

If Ω denotes the area of the photodetector, the demodulated signal is given by

$$\begin{aligned} S = {} & \frac{\epsilon_0 c}{2}\iint_\Omega \mathrm{d}x\mathrm{d}y p(x,y) \\ & \times [P(\eta,x,y)E^{\mathrm{CR}}(x,y)]^\dagger[P(\eta,x,y)E^{\mathrm{SB}-}(x,y)] \\ & + \frac{\epsilon_0 c}{2}\iint_\Omega \mathrm{d}x\mathrm{d}y p(x,y) \\ & \times [P(\eta,x,y)E^{\mathrm{SB}+}(x,y)]^\dagger[P(\eta,x,y)E^{\mathrm{CR}}(x,y)], \end{aligned} \tag{A12}$$

where $p(x,y)$ is a pupil-weighting function and where $E^{\mathrm{CR}}(x,y)$ and $E^{\mathrm{SB}\pm}(x,y)$ are the field amplitudes at the output of an optical system for the carrier and sidebands of the modulated light, respectively. $P(\eta,x,y)$ is the propagator between the output and the photodetector. In the modal space coordinates, the first term in Eq. (A12) becomes

$$\begin{aligned} & \frac{\epsilon_0 c}{2}\sum_{mn,kl}(E^{\mathrm{CR}}_{mn})^\dagger \exp[i(m+n+1)\eta] \\ & \times \iint_\Omega \mathrm{d}x\mathrm{d}y p(x,y)U^\dagger{}_{mn}(x,y,z)U_{kl}(x,y,z) \\ & \times \exp[i(k+l+1)\eta]E_{kl}{}^{\mathrm{SB}-}. \end{aligned} \tag{A13}$$

Comparing this expression with the definition of the demodulation operator in the modal space in Eq. (16) gives

$$D^\Omega_{mn,kl} = \iint_\Omega \mathrm{d}x\mathrm{d}y p(x,y)U^\dagger{}_{mn}(x,y,z)U_{kl}(x,y,z). \tag{A14}$$

When the photodetector size is constant relative to the beam spot size, the demodulation operator is independent of the position of the photodetector. For a full-plane detector the pupil-weighting function becomes $p(x,y) = 1$, and Eq. (A14) reduces to the orthonormality condition of Eq. (A3a), i.e.,

$$D^{\text{full-plane}}_{mn,kl} = \delta_{mk}\delta_{nl}. \tag{A15}$$

For a half-plane detector that is split along the y axis and where the signals from the two half-planes are subtracted from each other, the pupil-weighting function is $p(x,y) = 1$ for $x \geq 0$ and $p(x,y) = -1$ for $x < 0$. The integration can then be written as

$$\iint_\Omega \mathrm{d}x\mathrm{d}y p(x,y) \to \int_{-\infty}^{\infty}\mathrm{d}y\left(\int_0^\infty \mathrm{d}x - \int_{-\infty}^0 \mathrm{d}x\right). \tag{A16}$$

ACKNOWLEDGMENTS

We thank our colleagues on the LIGO project who helped us with many useful suggestions and comments. This work is supported by NSF grant PHY-9210038. D. Sigg was supported by the Swiss National Science Foundation.

*Present address, Elscint, Nuclear Medicine, Division R&D Dept., POB 550, Haifa 31004, Israel.

REFERENCES AND NOTES

1. K. S. Thorne, "Gravitational radiation," in *300 Years of Gravitation*, S. W. Hawking and W. Israel, eds. (Cambridge U. Press, Cambridge, 1987), Chap. 9, pp. 330–458.
2. A. Abramovici, W. E. Althouse, R. W. P. Drever, Y. Gursel, S. Kawamura, F. J. Raab, D. Shoemaker, L. Sievers, R. E. Spero, K. S. Thorne, R. E. Vogt, R. Weiss, S. E. Whitcomb, and M. E. Zucker, "LIGO: the Laser Interferometer Gravitational-Wave Observatory," Science **256**, 325–333 (1992).
3. M. W. Regehr, F. J. Raab, and S. E. Whitcomb, "Demonstration of a power-recycled Michelson interferometer with Fabry–Perot arms by frontal modulation," Appl. Opt. **20**, 1507–1509 (1995).
4. C. N. Man, D. Shoemaker, M. Pham Tu, and D. Dewey, "External modulation technique for sensitive interferometric detection of displacements," Phys. Lett. A **148**, 8–16 (1990).
5. A. Schenzle, R. DeVoe, and G. Brewer, "Phase-modulation laser spectroscopy," Phys. Rev. A **25**, 2606–2621 (1982).
6. R. W. P. Drever, J. L. Hall, F. V. Kowalski, J. Hough, G. M. Ford, A. J. Munley, and H. Ward, "Laser phase and frequency stabilization using an optical resonator," Appl. Phys. B **31**, 97–105 (1983).
7. L. Schnupp, Max Planck Institute for Quantum Optics, Garching, Germany (personal communication, 1986).
8. Y. Hefetz and N. Mavalvala, in "Sensitivity of the LIGO interferometer to mirror misalignment and method for automatic alignment," in *Proceedings of the Seventh Marcel Grossmann Meeting on General Relativity*, R. Ruffini, ed. (World Scientific, Singapore, 1996), pp. 1349–1351.
9. D. Z. Anderson, "Alignment of resonant optical cavities," Appl. Opt. **23**, 2944–2949 (1984).
10. N. Sampas and D. Z. Anderson, "Stabilization of laser beam alignment to an optical resonator by heterodyne detection of off-axis modes," Appl. Opt. **29**, 394–403 (1990).
11. E. Morrison, B. J. Meers, D. I. Robertson, and H. Ward, "Experimental demonstration of an automatic alignment system for optical interferometers," Appl. Opt. **33**, 5037–5040 (1994).
12. E. Morrison, B. J. Meers, D. I. Robertson, and H. Ward, "Automatic alignment of optical interferometers," Appl. Opt. **33**, 5041–5049 (1994).

13. J. Vinet, P. Hello, C. N. Man, and A. Brillet, "A high accuracy method for the simulation of non-ideal optical cavities," J. Phys. I (Paris) **2**, 1287–1303 (1992).
14. P. Saha, "Fast estimation of transverse fields in high-finesse optical cavities," J. Opt. Soc. Am. A (to be published).
15. A. E. Siegman, *Lasers* (University Science, Mill Valley, Calif., 1986), Chap. 13, p. 663.
16. An introduction to group theory can be found, e.g., in H. Georgi, *Lie Algebras in Particle Physics* (Benjamin Cummings, Menlo Park, Calif., 1982), Chap. 2, p. 8.
17. Note that the eigenvalues of $M(\Theta_x, \Theta_y)$ can exceed unity, if just first-order terms are included. To obtain numerically stable solutions, the terms of at least second order in Θ_i must be included, if M is to be used in Eq. (20).